WILEY | Hindawi

Research Article

A Study on the Effects of Loading Axial Pressure Rate on Coal Mechanical Properties and Energy Evolution Law

Hongjun Guo [1,2,3] **Zhongguang Sun** [4,5] **Ming Ji** [6] **Dapeng Liu** [1] **Lihui Nian,**[1] **and Yongfeng Wu**[1]

[1]*Jiangsu Vocational Institute of Architectural Technology, Xuzhou 221116, China*
[2]*Jiangsu Collaborative Innovation Center for Building Energy Saving and Construction Technology, Xuzhou, Jiangsu 221116, China*
[3]*State Key Laboratory for Geomechanics & Deep Underground Engineering, China University of Mining & Technology, Xuzhou 221116, China*
[4]*State Key Laboratory of The Gas Disaster Detecting, Preventing and Emergency Controlling, Chongqing 400037, China*
[5]*China Coal Technology and Engineering Group Chongqing Research Institute, Chongqing 400039, China*
[6]*Key Laboratory of Deep Coal Resource Mining, Ministry of Education of China, School of Mines, China University of Mining & Technology, Xuzhou 221116, China*

Correspondence should be addressed to Ming Ji; jiming@cumt.edu.cn

Due to the unique nature of the coal mining industry, safety is always one highly upheld premise of high production and high efficiency. According to the stress adjustment characteristics of the surrounding rocks in roadway excavation under a nondisruptive environment, the stress paths of unloading confining pressure and loading axial pressure were designed creatively and vividly, and the coal mechanical properties and energy evolution law under different loading axial pressure rates were studied through a series of experiments. As the loading axial pressure rate increases, the mechanical parameters at the time of coal failure show a nonlinear increase in the peak strength, the confining pressure, and the axial strain, while the variation laws of lateral strain and volumetric strain are not obvious. In addition, the failure mode transfers from the brittle failure to the ductile failure. In terms of energy, the positive work done by the axial pressure, the total work, and the elastic strain energy tend to increase nonlinearly, while the negative work done by the confining pressure and the plastic strain energy increase conversely. The elastic strain energy conversion rate increases logarithmically, indicating that a higher loading axial pressure rate tends to increase the probability and strength of coal instantaneous failure and subsequent dynamic behaviors. The research results reveal that providing an appropriate pressure relief and timely support after the roadway excavation in the actual production process can effectively reduce the energy level of the environment at the location of the surrounding rock support system, which is conducive to the roadway support and the surrounding rock stability control. Furtherly, it has important reference value for the roadway excavation and other underground engineering excavation and support operations and is of great significance to promote the development of deep resources.

1. Introduction

The deep resource development is considered as an important strategic direction after the deep sea, deep space, and deep blue in China, which is a scientific research highland pursued in the field of science and technology in the world [1, 2]. The relevant mechanical properties of engineering coal and rock mass serve as the foundation for the design, construction, and related disaster prevention of geotechnical and underground engineering and have always been favored by the scientific and technological workers all the time. In recent years, some studies have shown that in practical engineering, especially underground or mining engineering, the stress characteristics of excavation surrounding rock are more in line with the stress path of unloading confining pressure and axial loading [3–5]. Zhao [6] analyzed the rock

Figure 1: The coal specimen.

Figure 2: The 815.02 electro-hydraulic servo-controlled rock mechanics testing system.

mechanic principle of major deep engineering in details and discussed eight unsolved century-old problems of rock mechanics. Li et al. [7] systematically reviewed and analyzed the important research progress and deficiencies of unloading rock mass mechanics test from three aspects: indoor rock triaxial unloading test, engineering rock excavation unloading model test, and engineering rock field excavation unloading test. A series of granite rockburst experiments at different unloading rates were performed by He and Zhao [8], which indicates that unloading rate has great influence on failure modes of specimens. Guo et al. [9] investigated the influences of the unloading rate on the mechanical properties of siltstone through an experiment featured with a constant axial pressure and unloading confining pressure and concluded that a high unloading rate increased the risk of rockburst. Ji et al. [10] discussed the mechanism of the unloading-induced fracture activation through a series of experiments and proposed a new approach to estimate the maximum seismic moment. Wang et al. [11] analyzed the effects of various unloading rates, the initial confining pressure [12], and the unloading time on the tension-shear ratio through a granite experiment featured with the unloading confining pressure and loading axial pressure, along with the failure mechanism of excavation disturbance. Zhu et al. [13] and Qian et al. [14] mainly researched the influences of the unloading stress path, unloading rate, and unloading point. The existing studies have revealed that as high as 80% of the failure strength under the corresponding confining pressure is generally selected at the unloading point [15–18]. Under the same loading and unloading stress path, (1) a higher initial confining pressure tends to lead to more energy stored in the coal body and severer damages; (2) a higher unloading rate tends to lead to less energy stored in the coal body, which is more prone to brittle failure and the more complex the damage degree [19–21]; Xue et al. [19] indicated that the energy required for rock failure is a definite value under certain conditions and is not affected by the stress loading path. Regarding the researches on the engineering properties of excavation rock mass, in addition to the above-mentioned influencing factors, the loading axial pressure rate is also a critical factor and mainly reflects the speed of stress concentration in the construction environment. However, limited researches have been conducted in this regard. Feng et al. [22] found that the evolution law of deformation and permeability parameters is basically consistent with the change in loading and unloading rate in the stage of axial stress loading and confining pressure unloading. Currently, the research on the performance mechanism of loading axial pressure rate in the experiment of unloading confining pressure and loading axial pressure is very limited, resulting in the needs to be explored urgently.

Meanwhile, the coal consumption in China accounted for 56.0% of the total energy consumption in year 2021, indicating that coal is and will be still a dominating energy source in a certain period of time in the future [23]. Faced with the objective reality of the coal resources reduction or depletion and the actual consumption demand of a large proportion, the mining pattern has shifted to high buried depths, complex geological conditions, and high-intensity operations. However, the statistic has revealed that frequent accidents have seriously affected the safe and efficient production of mines [24–26]. The key to effectively solve the safety problem of deep resource development still lies in the engineering rock mechanics. Xie [27] and He [28] suggest that due to the strong construction disturbance, increased water inflow, the occurrence environment of the "three highs" (high ground stress, high temperature, and high osmotic pressure), and obvious time effect, the organizational structure, basic behavior characteristics, and engineering response of coal and rock mass have all undergone fundamental changes [29, 30]. Therefore, in this study, the deep coal unloading confining pressure and loading axial pressure experiment are considered together to explore the influences of the loading axial pressure rate in undistributed environment on the mechanical properties and energy evolution law of excavation surrounding rock [31], aiming to provide insights for the support design and surrounding rock stability control of roadway or other similar excavation projects.

2. Experimental Overviews

2.1. Experiment Preparation. The coal samples were selected from the #8 coal seam of a mine located in Xianyang, Shanxi Province. According to the production standard of coal-rock mechanics specimens, the coal samples were processed into cylindrical specimens in a dimension of $\Phi 50 \, \text{mm} \times \text{H}100$ mm, as shown in Figure 1. The experiment was completed by adopting the 815.02 electro-hydraulic servo-controlled rock mechanics testing system (as shown in Figure 2), in the State Key Laboratory for Geomechanics & Deep
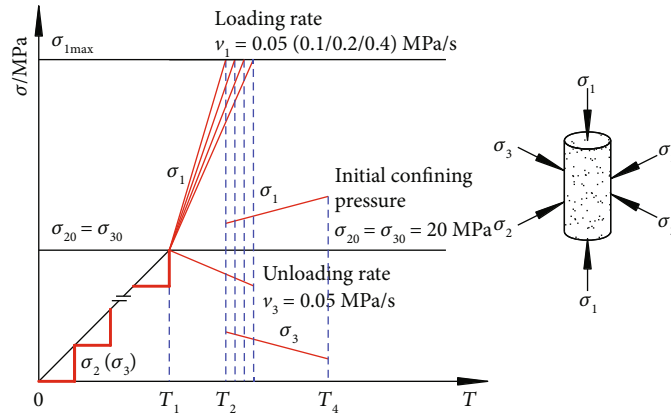
FIGURE 3: Stress path of unloading confining pressure and loading axial pressure.

TABLE 1: Test results.

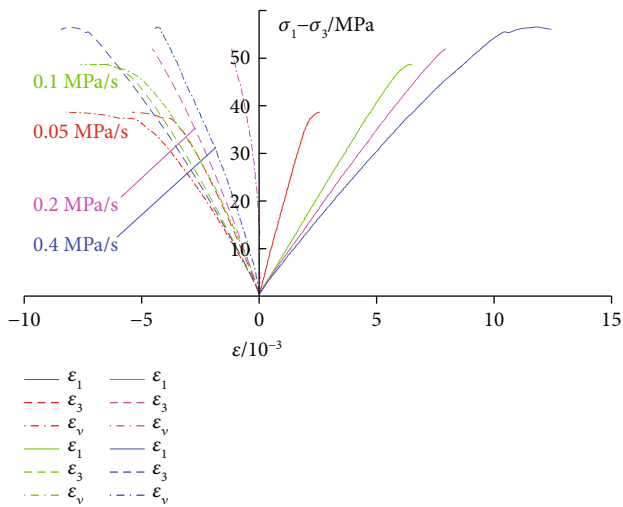| Number	Loading axial pressure rate v_1/(MPa/s)	Lateral strain ε_3/10^{-3}	Volume strain ε_v/10^{-3}	Confining pressure σ_3/MPa	Axial strain ε_1/10^{-3}	Failure strength σ_c/MPa	Average failure strength $\overline{\sigma}_c$/MPa
1	0.05	-5.409	-8.234	1.107	2.585	39.755	
2	0.05	-5.909	-9.024	0.023	2.794	41.227	39.317
3	0.05	-6.542	-10.133	3.451	2.952	36.969	
4	0.1	-3.845	-3.317	8.205	4.374	44.802	
5	0.1	-6.458	-6.549	4.155	6.367	52.851	53.159
6	0.1	-4.830	-3.769	3.358	5.892	54.071	
7	0.2	-4.551	-1.147	9.804	7.954	61.750	
8	0.2	-8.235	-7.519	8.600	8.951	67.611	60.879
9	0.2	-4.691	-2.550	11.977	6.832	53.275	
10	0.4	-4.170	-0.781	15.755	7.578	55.432	
11	0.4	-8.169	-4.961	14.543	11.378	65.524	63.814
12	0.4	-8.102	-4.360	13.929	11.845	70.485	

FIGURE 4: The stress-strain curves.

Underground Engineering, China University of Mining & Technology.

2.2. Experimental Scheme. In the engineering, the construction stress environment generally refers to the original rock area or construction disturbance area. The experiment does not consider the influence of construction disturbance, aiming to simulate the force change of surrounding rock during the excavation of the solid coal roadway. With the burial depth of 800 m for the #8 coal seam, the initial confining pressure is set at 20 MPa in the experiment, in other words, when the coal specimen is in the original rock state of 20 MPa, the axial pressure is loaded, and the confining pressure is unloaded until the failure. Considering the average uniaxial compressive strength of coal body is 22.3 MPa, the design of loading and unloading stress path are shown in Figure 3. The specific implementation process is provided as follows:

(a) Failure strength and confining pressure

(b) Strain

UCPLAP-unloading confining pressure and loading axial pressure;
CTC-conventional triaxial compression

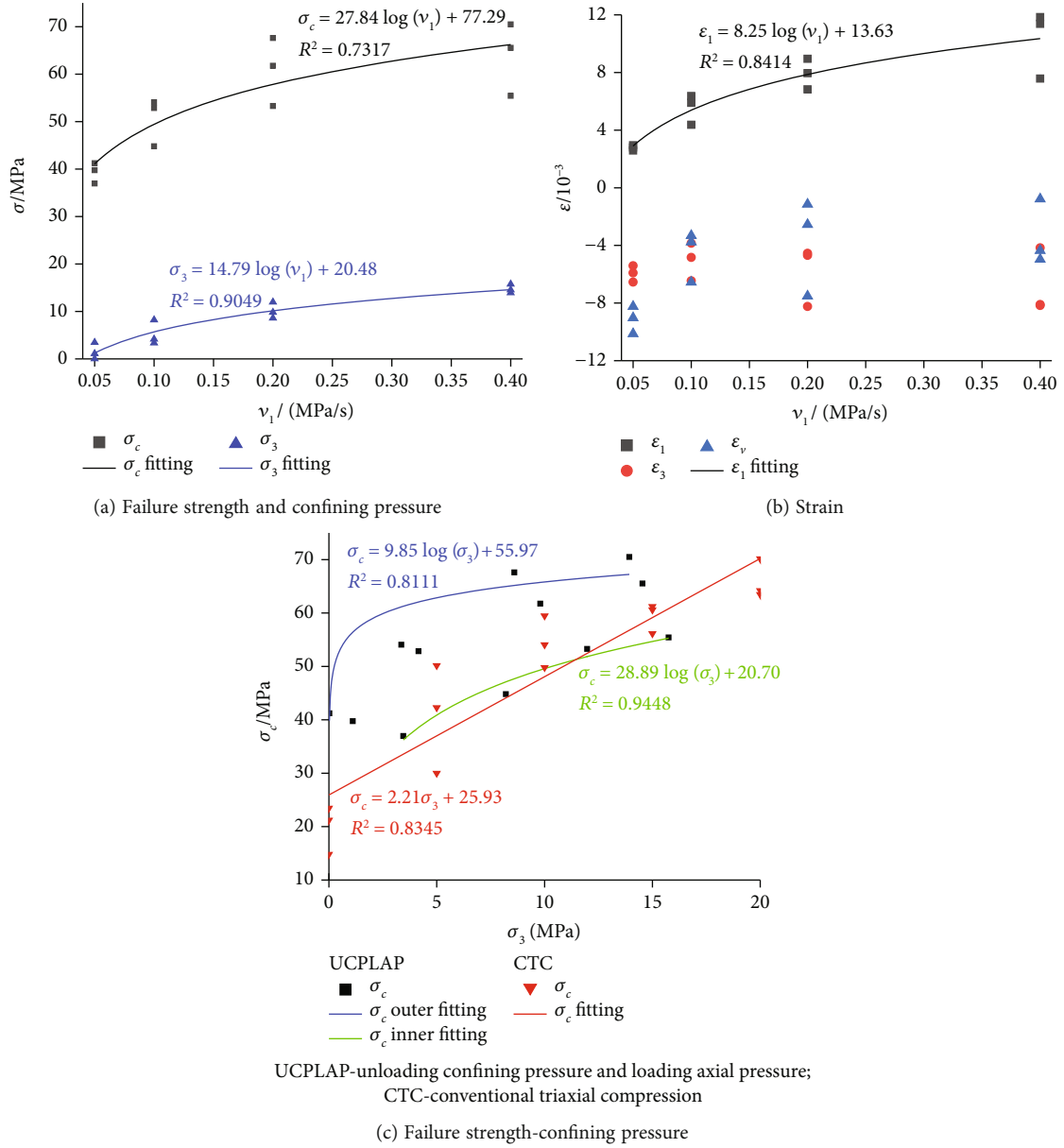(c) Failure strength-confining pressure

FIGURE 5: The relationship among stress, strain, and loading axial pressure rate. UCPLAP: unloading confining pressure and loading axial pressure; CTC: conventional triaxial compression.

(1) Under the stress control mode, the loading rate is set at 0.05 MPa/s, with the confining pressure σ_3 and axial pressure σ_1 alternately loaded every 5 MPa to 20 MPa

(2) Under the stress control mode, the confining pressure σ_3 is unloaded at $v_3 = 0.05$ MPa/s, and simultaneously, the axial pressure σ_1 is loaded with $v_1 = 0.05$ MPa/s (0.1 MPa/s, 0.2 MPa/s, and 0.4 MPa/s) until the coal sample fails

(3) Under the displacement control mode, the unloading rate v_3 and the loading rate v_1 are set at 0.001 mm/s, with the confining pressure σ_3 and axial

pressure σ_1 simultaneously conducted to obtain the full stress-strain curve

3. Results and Discussion

The deformations and failures of coal body under different loading axial pressure rates are shown in Table 1.

3.1. The Relationship between the Loading Axial Pressure Rate and Mechanical Properties of the Coal Body. Taking some typical specimens as an example, Figure 4 shows the stress-strain relationship of the typical coal specimens under different loading axial pressure rates.
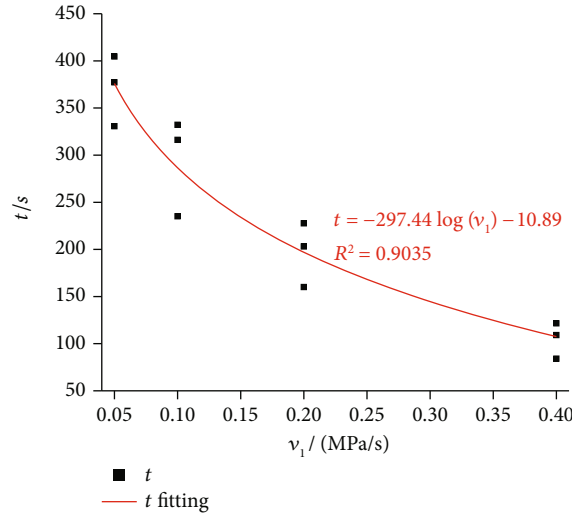
FIGURE 6: Relationship between failure time and loading axial pressure rate.

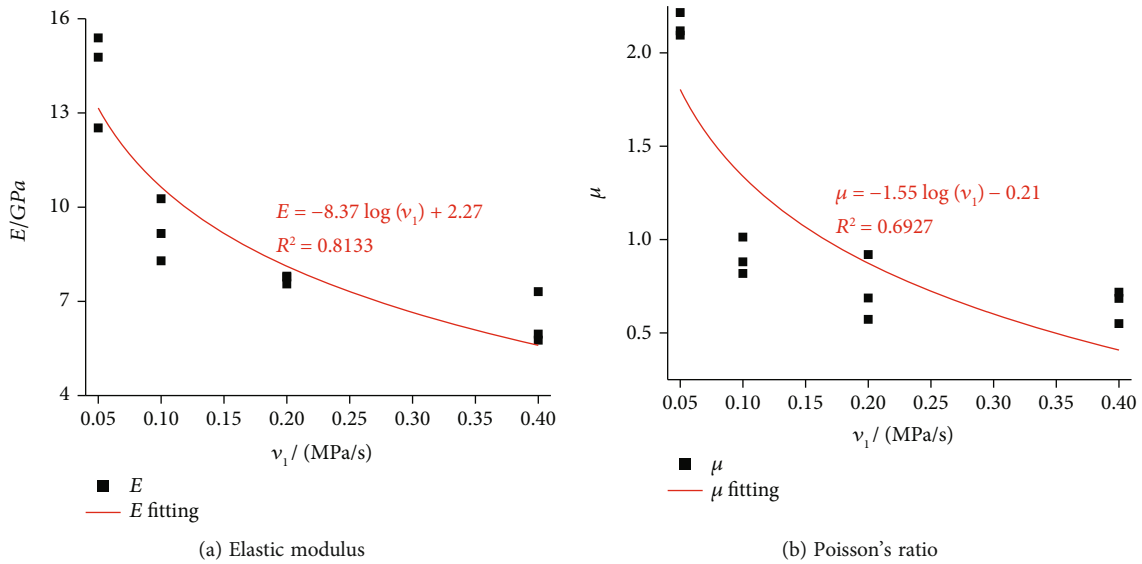(a) Elastic modulus

(b) Poisson's ratio

FIGURE 7: The relationship between deformation parameters and loading axial pressure rate.

According to Figure 4, the unloading shows good linear elastic characteristics at the initial stage due to the coal body at the unloading point in a natural compaction state. The coal body continues to unload and gradually enters the plastic state until the failure. Taking Figure 5 into consideration, as the loading axial pressure rate increases, the strength, confining pressure, and axial strain of coal body at failure show an upward trend, while the variation law of lateral strain and volumetric strain is not obvious. In Figure 5(c), the failure strength of coal body increases logarithmically with the (residual) confining pressure as a whole, and fluctuates between the inner and outer fitting lines. And compared with the conventional triaxial compression strength of coal body, increasing the loading axial pressure rate within a certain range can strengthen the coal body, which can be explained by the rapid load axial pressure reflecting the failure strength under the condition of high confining pressure. Meanwhile, the loading action on the coal body is controlled short and insufficient, resulting in low development degree of internal microcracks and very limited damage accumulation. When the bearing limit of the coal body is reached and exceeded, the main failure crack is formed instantaneously, and the failure occurs. Therefore, a rapid load axial pressure tends to improve the failure strength of the coal body under the corresponding confining pressure to a certain extent.

Figure 6 shows the failure time of coal body under different loading axial pressure rates. As shown in Figure 6, a greater loading axial pressure rate often leads to a shorter failure time. Combined with Figure 5(c), the strengthening effect of increasing the loading axial pressure rate on coal body is gradually weakened. When the threshold is reached, to some extent, the mechanical properties of coal body from axial compression to failure under the approximate initial confining pressure state are manifested. At this point, the difference is mainly caused by the differences in the specimens themselves.

(a) The work of axial pressure U_1

(b) The work of confining pressure U_3

(c) The total work U

(d) The elastic strain energy w_e

(e) The plastic strain energy w_d

(f) Energy and loading axial pressure rate

In panel (f):
$U_1 = 0.43 \log(v_1) + 0.63$
$R^2 = 0.7685$

$U = 0.27 \log(v_1) + 0.45$
$R^2 = 0.7788$

$w_e = 0.31 \log(v_1) + 0.46$
$R^2 = 0.7736$

$w_d = -0.037 \log(v_1) - 0.008$
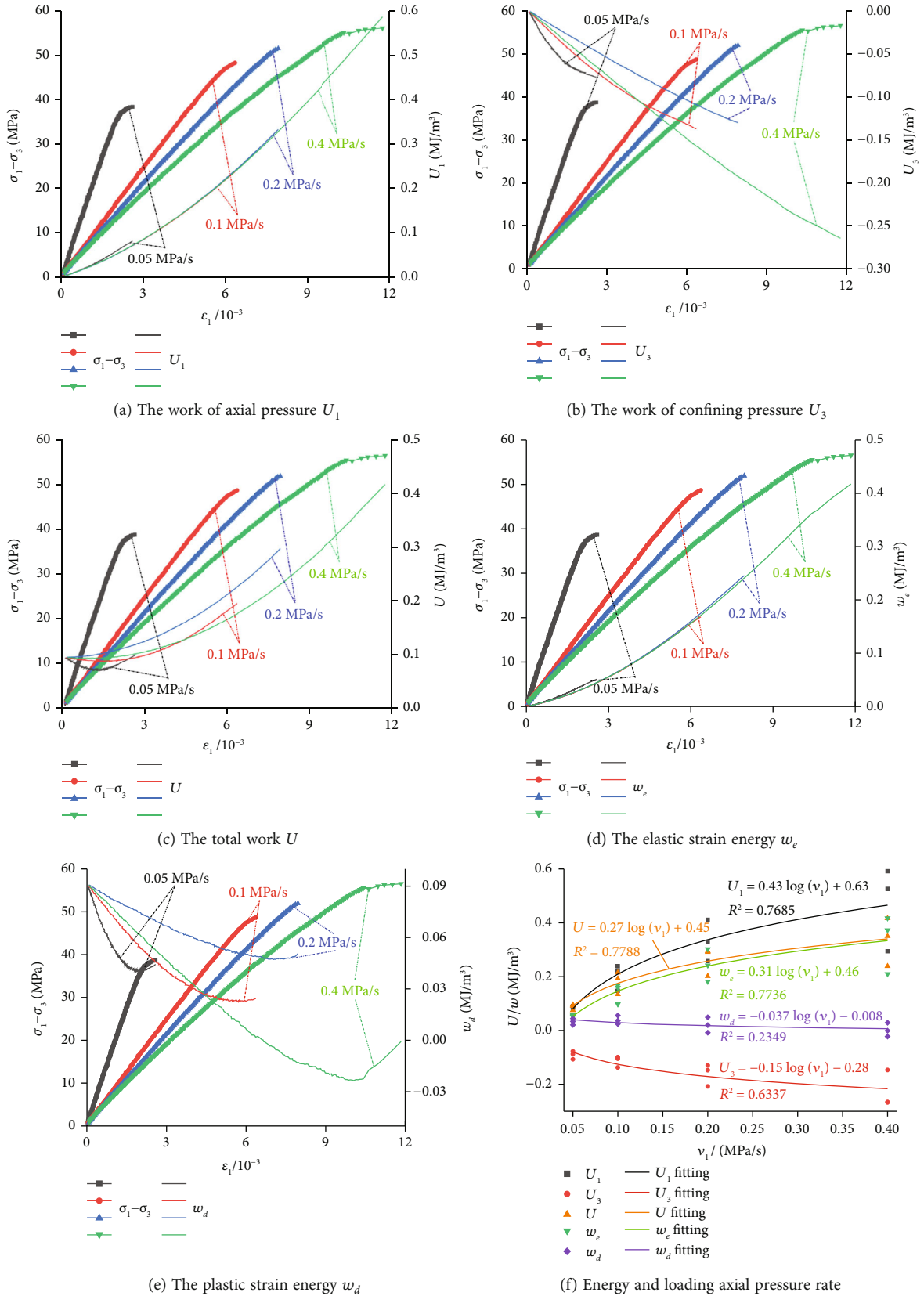$R^2 = 0.2349$

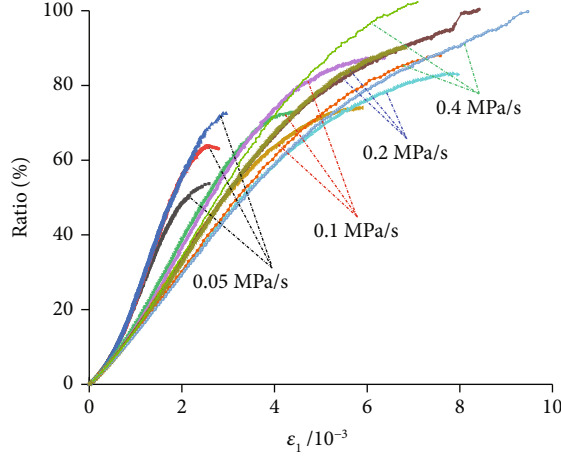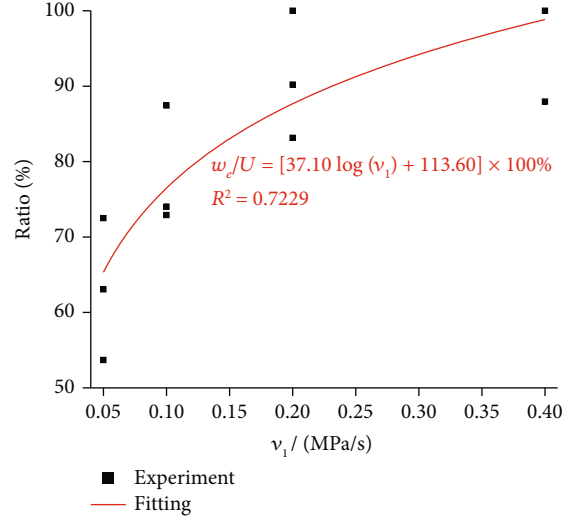$U_3 = -0.15 \log(v_1) - 0.28$
$R^2 = 0.6337$

FIGURE 8: Energy evolution curves.

(a) Elastic energy evolution curves

(b) The conversion rate of elastic strain energy and loading axial pressure rate

FIGURE 9: Elastic strain energy conversion ratios.

At the failure, the relationship between the deformation parameters and the loading axial pressure rate of the coal body is shown in Figure 7.

Figure 7 shows that the elastic modulus and Poisson's ratio decrease nonlinearly with the increase of loading axial pressure rate. In this study, the circumstances under the Poisson's ratio greater than 0.5 are not discussed. The decrease of elastic modulus contributes to the occurrences of the coal body deformation. In addition, the positive correlation between axial strain and loading axial pressure rate in Figure 5(b) provides a similar conclusion. However, under the condition of a high loading axial pressure rate, the coal body is in a state of higher triaxial compressive stress, and its failure strength is higher. Although the ductility characteristics of coal body are enhanced, the dynamic failure phenomenon is still prone to occur in the near failure process. This is related to the stress path of loading and unloading and the loading axial pressure rate.

3.2. The Relationship between the Loading Axial Pressure Rate and Energy Evolution of Coal Body. Assuming that the total work U performed by the test system during the process of unloading confining pressure and loading axial pressure is generated by the axial pressure and confining pressure, and only transformed into elastic strain energy w_e and plastic strain energy w_d, it can be expressed as

$$U = U_1 + U_3 = w_e + w_d, \tag{1}$$

where $U_1 = \int_0^{\varepsilon_{1(t)}} \sigma_1 d\varepsilon_1$, $U_3 = 2\int_0^{\varepsilon_{3(t)}} \sigma_3 d\varepsilon_3$, and $w_e = (1/2)\sigma_1\varepsilon_1$.

Since the unloading point is in the state of 20 MPa hydrostatic pressure, a large amount of energy has been stored in the coal body, indicating that the original rock energy stores in a natural state. Combined with the conventional triaxial compression experiment and the experimental data of alternate loading of confining pressure and axial pressure before unloading, the average original rock energy

storage w_0 under such condition is 0.0912 MJ/m³. Therefore, Equation (1) can be rewritten into

$$U = w_0 + U_1 + U_3 = w_e + w_d. \tag{2}$$

The experimental data was substituted into the Equation (2) to obtain the energy evolution of coal body under different loading axial pressure rates. The energy evolution process of some typical specimens is shown in Figure 8.

According to Figures 8(a)–8(e), with the increase of loading axial pressure rate, the positive work U_1 done by the axial pressure, total work U, and elastic strain energy w_e all show an upward trend, while the regularity of the negative work U_3 done by the confining pressure and the plastic strain energy w_d is relatively low due to the data at $v_1 = 0.2$ MPa/s. Figure 8(f) shows the approximate logarithmic relationship between each energy and the loading axial pressure rate at the coal failure, which is consistent with the aforementioned conclusion. At the same time, the negative work U_3 tends to increase while w_d decreases. Under the condition of low loading axial pressure rate, the test system inputs less energy to coal body per unit time, resulting in longer time consumption to reach the energy storage limit of coal body under a certain confining pressure, providing conditions for long-term driving action of energy for crack development and microdamage accumulation in the coal body. With the increase of loading axial pressure rate, the coal body tends to reach the failure in a faster manner, with a low damage accumulation. Therefore, the plastic strain energy decreases with the increase of loading axial pressure rate, while the elastic strain energy demonstrates an opposite trend. Similar to the changes of mechanical properties of coal body, each energy evolution amplitude gradually decreases and tends to be stable with the increase of loading axial pressure rate. At the threshold, the energy changes from the compression into the failure under initial confining

(a) Excavation unloading
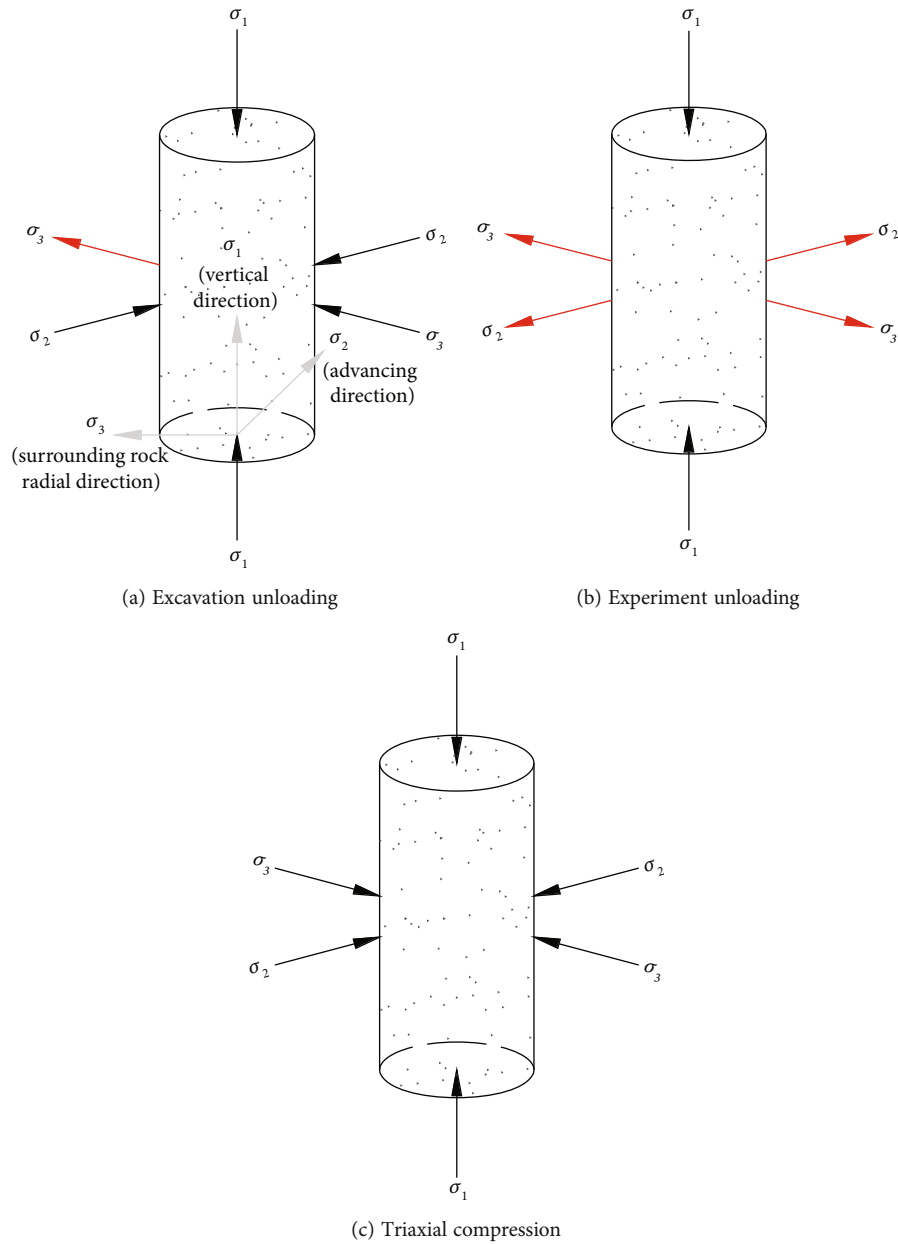
(b) Experiment unloading

(c) Triaxial compression

FIGURE 10: Comparison of excavation unloading and experiment unloading.

pressure. At this point, the internal energy differences of coal body are mainly caused by the specimen itself.

According to relevant researches on rockburst or impact of coal and rock mass, a higher releasable elastic strain energy stored in the coal body can lead to a greater possibility and risk of dynamic failure of coal and rock mass. Figure 9 shows the evolution process of elastic strain energy and the conversion rate at failure time of coal specimen under different loading axial pressure rates.

According to Figure 9(a), the ratio of the input energy of the test system into elastic strain energy increases approximately linearly at the initial stage of unloading (elastic stage) and then slowly increases to fluctuating change (plastic stage). Figure 9(b) clearly reflects that the conversion rate of elastic strain energy at the time of coal failure increases logarithmically with the increase of loading axial pressure rate. Therefore, the probability of coal dynamic behavior increases under the condition of high loading axial pressure rate. Loading axial pressure at a higher rate tend to shorten the time from unloading to failure, but retain the triaxial compression environment closer to the initial confining pressure, resulting in a higher energy input to reach the energy storage limit of coal body. The plastic strain energy is mainly dissipated by forming the main failure crack and accounts for a low proportion of the total input energy. Therefore, under most circumstances, the input energy is

stored in the form of elastic strain energy and released instantaneously at the failure time, which not only shows strong failure characteristics but also has a much greater probability and strength of subsequent dynamic behavior of failure than that under low-speed load axial pressure.

3.3. Discussion. The unloading path and evolution process of the coal body in the original rock state in the experiment are still different from the actual excavation unloading, which is not completely consistent, as shown in Figure 10.

In the actual excavation process, the studied coal body is restrained by the surrounding rock along the axial and radial deep of the roadway with the unloading mainly occurs on the side of the free space of the roadway (as shown in Figure 10(a)), resulting in some uneven confining pressure constraints in the circumferential direction. During the experiment, the coal body was overall unloaded in the circumferential direction (Figure 10(b)), resulting in the uniform confining pressure constraints at all times. When the loading axial pressure rate is significantly higher than the unloading rate, the experimental stress path can evolve into axial loading under high confining pressure in a short time (Figure 10(c)). A greater loading axial pressure rate can lead to a closer circumferential confining pressure constraint to the initial confining pressure.

Taking the experimental results into consideration, the following conclusions can be drawn. (1) Compared with the experimental coal body, less negative work was done by the confining pressure to the surrounding rock (shallow) coal body in the actual excavation roadway, and the internal energy storage of coal body increases rapidly under the condition of equal loading axial pressure rate. The internal deterioration before the failure of coal body and the dynamic behavior at the failure time of coal body tend to be more obvious. (2) In actual production, the roadway support is considered as the most important method to maintain the stability of surrounding rock, which depends on the support timing. Appropriate unloading and timely support after roadway excavation can transform the surrounding rock support system from a low-energy environment into an affordable high-energy environment in the process of stabilization. The immediate support after excavation tends to place the surrounding rock support system in a high-energy environment at the initial stage, resulting in more input energy during the stabilization process. When the environmental energy storage exceeds the bearing limit of the surrounding rock support system, some strong ground pressure behaviors and even a certain scale of rock burst can take place. The former is like a low-speed load axial pressure, which has a certain time to achieve confining pressure drop, while the latter is similar to the high-speed load axial pressure, which is more likely to cause dynamic accidents [32–34].

4. Conclusions

The stress path of unloading confining pressure and loading axial pressure is in line with the stress adjustment process of surrounding rock in the undisturbed general excavation of underground engineering (such as solid coal roadway excavation). Based on the experiment, the effect of loading axial pressure rate on the mechanical characteristics and energy evolution law of coal body is analyzed, with the following conclusions obtained:

(1) As the loading axial pressure rate increases, the peak strength, confining pressure, and axial strain increase at the time of coal failure, while the variation laws of lateral strain and volumetric strain are not obvious; meanwhile, stress environment of coal body evolves to axial compression under near initial confining pressure with the failure mode evolving from the brittle failure to the ductile failure

(2) As the loading axial pressure rate increases, the positive work done by the axial pressure, total work, and elastic strain energy increase, while the negative work done by the confining pressure and plastic strain energy decrease. The energy evolution inside the coal body becomes less dramatic, until the stabilization. The elastic strain energy conversion rate increases in logarithmic form, which increases the probability and strength of instantaneous failure and subsequent dynamic behavior under high-speed loading

(3) Some differences between the stress adjustment of surrounding rock in actual excavation and the unloading of pseudotriaxial experiment have been noticed. Under the same condition, the internal deterioration before coal failure and the dynamic behavior at the coal failure time of the former tend to be more significant. According to the experiment, some appropriate pressure relief and timely support after roadway excavation can reduce the risk of dynamic disasters to some extent

Data Availability

The data used to support the findings of the study are available from the corresponding author upon request.

Conflicts of Interest

The authors declare that no conflict regarding the publication of this paper has been identified.

Acknowledgments

References

[1] Strategic Consulting Center of Chinese Academy of Engineering, Underground Space Branch of Chinese Society of Rock Mechanics and Engineering, China Urban Planning Society, *2021 Blue Book on Urban Underground Space Development in China (Public Edition)*, 2021, http://www.planning.org.cn/uploads/ueditor/php/upload/file/20211226/1640497942495762.pdf.

[2] H. Xie, F. Gao, Y. Ju, R. Zhang, M. Gao, and H. Deng, "Novel idea and disruptive technologies for the exploration and research of deep earth," *Advanced Engineering Sciences*, vol. 1, no. 49, pp. 1–8, 2017.

[3] J. Lau and N. Chandler, "Innovative laboratory testing," *International Journal of Rock Mechanics and Mining Science*, vol. 41, no. 8, pp. 1427–1445, 2004.

[4] Y. Zhao, J. Bi, C. Wang, and P. Liu, "Effect of unloading rate on the mechanical behavior and fracture characteristics of sandstones under complex triaxial stress conditions," *Rock Mechanics and Rock Engineering*, vol. 54, no. 9, pp. 4851–4866, 2021.

[5] H. Guo, M. Ji, D. Liu, M. Liu, G. Li, and J. Chen, "An experimental research on surrounding rock unloading during solid coal roadway excavation," *Geofluids*, vol. 2021, Article ID 5604642, 9 pages, 2021.

[6] Y. Zhao, "Retrospection on the development of rock mass mechanics and the summary of some unsolved centennial problems," *Chinese Journal of Rock Mechanics and Engineering*, vol. 40, no. 7, pp. 1297–1336, 2021.

[7] J. Li, T. Huang, H. Zhang, and H. Deng, "Research review and prospect in experimental studies for unloading rock mass mechanics," *Journal of China Three Gorges University (Natural Sciences)*, vol. 44, no. 1, pp. 1–13, 2022.

[8] M. He and F. Zhao, "Laboratory study of unloading rate effects on rockburst," *Disaster Advances*, vol. 6, no. 9, pp. 11–18, 2013.

[9] H. Guo, M. Ji, and L. Cao, "Effect of unloading rate on the mechanical properties of siltstone," *Journal of Xi'an University of Architecture and Technology (Natural Science Edition)*, vol. 52, no. 6, pp. 860–868, 2020.

[10] Y. Ji, W. Wu, and Z. Zhao, "Unloading-induced rock fracture activation and maximum seismic moment prediction," *Engineering Geology*, vol. 262, p. 105352, 2019.

[11] C. Wang, H. Zhou, R. Wang, Z. Wang, S. He, and J. Liu, "Failure characteristics of Beishan granite under unloading confining pressures," *Chinese Journal of Geotechnical Engineering*, vol. 41, no. 2, pp. 329–337, 2019.

[12] Q. Fang, L. Shang, Y. Shang, and Z. Chen, "Mechanical and energy characteristics of granites under unloading test," *Journal of Central South University (Science and Technology)*, vol. 47, no. 12, pp. 4148–4153, 2016.

[13] Z. Zhu, L. Yu, J. Li, Q. Meng, B. Sui, and Z. Zhang, "Deformation evolution and dissipated energy characteristics of marble under pre-peak unloading conditions," *Journal of China Coal Society*, vol. 45, no. S1, pp. 181–190, 2020.

[14] Y. Qian, Y. Wu, W. Pei, and Y. Zhu, "Rock strength and deformation characteristics under different unloading rates," *Hydro-Science and Engineering*, vol. 6, pp. 48–54, 2020.

[15] T. Qin, H. Sun, H. Liu et al., "Experimental study on mechanical and acoustic emission characteristics of rock samples under different stress paths," *Shock and Vibration*, vol. 2018, Article ID 4813724, 9 pages, 2018.

[16] K. Du, M. Tao, X. Li, and J. Zhou, "Experimental study of slabbing and rockburst induced by true-triaxial unloading and local dynamic disturbance," *Rock Mechanics and Rock Engineering*, vol. 49, no. 9, pp. 3437–3453, 2016.

[17] G. Zhao, B. Dai, L. Dong, and C. Yang, "Energy conversion of rocks in process of unloading confining pressure under different unloading paths," *Transactions of Nonferrous Metals Society of China*, vol. 25, no. 5, pp. 1626–1632, 2015.

[18] B. Dai, G. Zhao, L. Dong, and C. Yang, "Mechanical characteristics for rocks under different paths and unloading rates under confining pressures," *Shock and Vibration*, vol. 2015, Article ID 578748, 8 pages, 2015.

[19] J. Xue, X. Du, Q. Ma, and K. Zhan, "Experimental study on law of limit storage energy of rock under different confining pressures," *Arabian Journal of Geosciences*, vol. 14, no. 1, pp. 1–8, 2021.

[20] Y. Guo, L. Wang, and X. Chang, "Study on the damage characteristics of gas-bearing shale under different unloading stress paths," *PLoS One*, vol. 14, no. 11, pp. 1–14, 2019.

[21] Y. Zhang, Y. Yang, and D. Ma, "Mechanical characteristics of coal samples under triaxial unloading pressure with different test paths," *Shock and Vibration*, vol. 2020, Article ID 8870821, 10 pages, 2020.

[22] K. Feng, K. Wang, D. Zhang, and Y. Yang, "Experimental study on mechanical properties and seepage laws of raw coal under variable loading and unloading rates," *Geofluids*, vol. 2021, Article ID 5596858, 9 pages, 2021.

[23] National Bureau of Statistics, *Statistical Bulletin of the People's Republic of China on National Economic and Social Development in 2021*, 2022, http://www.stats.gov.cn/tjsj/zxfb/202202/t20220227_1827960.html.

[24] Y. Xue, J. Liu, P. Ranjith, Z. Zhang, F. Gao, and S. Wang, "Experimental investigation on the nonlinear characteristics of energy evolution and failure characteristics of coal under different gas pressures," *Bulletin of Engineering Geology and the Environment*, vol. 81, no. 1, p. 38, 2022.

[25] Y. Xue, J. Liu, X. Liang, S. Wang, and Z. Ma, "Ecological risk assessment of soil and water loss by thermal enhanced methane recovery: numerical study using two-phase flow simulation," *Journal of Cleaner Production*, vol. 334, article 130183, 2022.

[26] X. Chen, L. Li, L. Wang, and L. Qi, "The current situation and prevention and control countermeasures for typical dynamic disasters in kilometer-deep mines in China," *Safety Science*, vol. 115, pp. 229–236, 2019.

[27] H. Xie, "Research review of the state key research development program of China: deep rock mechanics and mining theory," *Journal of China Coal Society*, vol. 44, no. 5, pp. 1283–1305, 2019.

[28] M. He, "Research progress of deep shaft construction mechanics," *Journal of China Coal Society*, vol. 46, no. 3, pp. 726–746, 2021.

[29] Y. Xue, J. Liu, P. Ranjith, F. Gao, H. Xie, and J. Wang, "Changes in microstructure and mechanical properties of low-permeability coal induced by pulsating nitrogen fatigue fracturing tests," *Rock Mechanics and Rock Engineering*, pp. 1–20, 2022.

[30] Y. Xue, P. Ranjith, Y. Chen, C. Cai, F. Gao, and X. Liu, "Non-linear mechanical characteristics and damage constitutive model of coal under CO_2 adsorption during geological sequestration," *Fuel*, vol. 331, article 125690, 2023.

[31] C. Dong, G. Zhao, X. Lu, X. Meng, Y. Li, and X. Cheng, "Similar simulation device for unloading effect of deep roadway excavation and its application," *Journal of Mountain Science*, vol. 15, no. 5, pp. 1115–1128, 2018.

[32] C. Xia, C. Xu, and S. Du, "Interaction between viscoelastic-plastic surrounding rock and support structure in deep tunnels considering stress path," *Chinese Journal of Rock Mechanics and Engineering*, vol. 40, no. 9, pp. 1789–1802, 2021.

[33] Z. Chen, X. Zhu, D. Zhao, and Y. Wang, "Research on anchorage mechanism of yielding support in the deep-buried tunnel," *Modern Tunnelling Technology*, vol. 56, no. 4, 2019.

[34] B. Wang, X. Guo, C. He, and D. Wu, "Analysis on the characteristics and development trends of the support technology of high ground stress tunnels in China," *Modern Tunnelling Technology*, vol. 55, no. 5, pp. 1–10, 2018.